Supporting Information
Dynamics of hydrogen bonds in the secondary structures of allosteric protein *Avena Sativa* phototropin 1

Mayar Tarek Ibrahim[1], Francesco Trozzi[1], and Peng Tao*[1]

[1]Department of Chemistry, Center for Research Computing, Center for Drug Discovery, Design, and Delivery (CD4), Southern Methodist University, Dallas, Texas, United States of America

The stability of the protein during the simulations was assessed by calculating the RMSD, for which the first frame of each simulation for the different configurations was the reference structure. RMSD was calculated over the time course of 500 ns, representing one of the three independent simulations performed for each configuration.

The trajectories of the light state configurations showed higher RMSD values up to 3Å (Figure S1a) than the dark state configurations with RMSD values fluctuating around 2Å from 100 ns to 500 ns (Figure S1b). This reflects that the light states have enhanced structural flexibility than the dark states. The mutant L408D in the transient light state configuration shows higher RMSD value of nearly 5Å.

A previous study identifies mutations that alter AsLOV2 photocycle by either enhancing or disrupting the helicity of A'α helix. The selected helicity-diminishing mutants L408D and R410P and one selected helicity-enhancing mutant T406A display similar RMSD range up to 3Å) (Figure S1).

Both the helicity-enhancing mutations and helicity-disrupting mutations (Figure S1) shared the same range of RMSD values (0Å to nearly 3Å), except for the mutant T407A in the transient light state configuration that showed a spike in the RMSD values around 200 ns.

Table S1: Secondary structure property for residues in the A'α helix based three independent simulations for each configuration. The secondary structure assignment is based on the dominant conformation that the residue adopts over the simulation ('H' denotes Alpha helix and 'C' denotes Coil)

Residue number	Light	Tslight	T406A tslight	T407A tslight	L408D tslight	R410P tslight
4	H	H	C	H	C	C
5	H	H	H	H	C	C
6	H	H	H	H	C	C
7	C	H	C	C	C	C
8	C	C	C	C	C	C
9	C	C	C	C	C	C
Residue number	Dark	Tsdark	T406A tsdark	T407A tsdark	L408D tsdark	R410P tsdark
4	H	H	H	C	C	C
5	H	H	H	H	C	C
6	H	H	H	H	C	C
7	H	H	H	H	C	C
8	C	C	C	C	C	C
9	C	C	C	C	C	C

Table S2: Hydrogen bond analysis using Baker-Hubbard method. Hydrogen bond is identified based on both distance (smaller than 2.5Å) and angle (larger than 120°)

Light	Tslight	T406A tslight	T407A tslight	L408D tslight	R410P tslight
THR406-N - PHE403-OY	THR406-N – PHE403-OY	ALA405-N – PHE403-OY	THR406-N – GLU409-OE1	ASP408-N – THR406-OG1	THR406-OG1 – PHE403-O
THR406-OG1 – GLU409-OE1	THR406-N – GLU409-OE1	ALA406-N – PHE403-OY	THR406-N – GLU409-OE2	GLU409-N – THR406-O	THR407-N – THR406-OG1
THR406-OG1 – GLU409-OE2	**THR407-OG1 – PHE403-O**	ALA406-N – PHE403-O	GLU409-N – THR406-O	**ARG410-N – THR406-O**	**THR407-OG1 – ALA542-O**
THR407-N – PHE403-O	**THR407-OG1 – ALA542-O**	**THR407-N – PHE403-OY**	ARG410-N – THR406-O	**ARG410-N – THR407-O**	LEU408-N – ALA405-O
THR407-OG1 – ALA542-O	**THR407-N – PHE403-O**	**THR407-OG1 – GLU545-OE1**	ARG410-N – ALA407-O	ARG410-NE – ALA405-O	GLU409-N – THR406-O
LEU408-N – LEU404-O	LEU408-N – LEU404-O	**THR407-OG1 – GLU545-OE2**	ARG410-NE – ALA405-O	ARG410-NH2 – GLU409-OE1	ILE411-N – LEU408-O
GLU409-N – ALA405-O	GLU409-N – ALA405-O	GLU409-N – ALA405-O	ARG410-NH1 – ALA405-O	LYS413-N – ILE411-O	
GLU409-N – THR406-O	GLU409-N – THR406-OG1	GLU409-N – ALA406-O	**ARG410-NH1 – GLU545-OE1**		
ARG410-N – THR406-O	GLU409-N – THR406-O	ARG410-N – ALA406-O	**ARG410-NH1 – GLU545-OE2**		
ARG410-N – THR407-O	**ARG410-N – THR406**-O	**ARG410-N – THR407**-O	ARG410-NH2 – ALA405-O		
ARG410-NH1 – GLU545-OE1	**ARG410-N – THR407**-O	ARG410-NE – ALA405-O	**ARG410-NH2 – GLU545-OE1**		
ARG410-NH1 – GLU545-OE2	**ARG410-NH1 – GLU545-OE1**	ARG410-NH2 – ALA405-O	**ARG410-NH2 – GLU545-OE2**		
ARG410-NH2 – GLU545-OE1	**ARG410-NH1 – GLU545-OE2**	ILE411-N – LEU408-O	ILE411-N – LEU408-O		
ARG410-NH2 – GLU545-OE2	ARG410-NH2 – ALA405-O				
ILE411-N – THR407-O	**ARG410-NH2 – GLU545-OE1**				
ILE411-N – LEU408-O	**ARG410-NH2 – GLU545-OE2**				
	ILE411-N – THR407-O				
	ILE411-N – LEU408-O				

Dark	Tsdark	T406A tsdark	T407A tsdark	L408D tsdark	R410P tsdark
ALA405-N – GLU409-OE1	THR406-N – GLU409-OE1	LEU404-N – ALA542-O	THR406-N – GLU409-OE1	THR406-OG1 – GLU409-OE1	**PHE403-N – THR406-O**
ALA405-N – GLU409-OE2	THR406-N – GLU409-OE2	ALA406-N – PHE403-OY	THR406-OG1 – PHE403-O	**THR407-OG1 – ALA542-O**	**ALA542-O – THR407-O**
THR406-N – GLU409-OE1	**THR407-OG1 – ALA542-O**	**THR407-N – PHE403-O**	THR406-OG1 – GLU409-OE1	GLU409-N – THR406-O	
THR406-N – GLU409-OE2	GLU409-N – ALA405-O	**THR407-OG1 – PHE403-O**	GLU409-N – THR406-OG1	**ARG410-N – THR406**-O	
THR407-OG1 – GLU545-OE1	GLU409-N – THR406-OG1	LEU408-N – LEU404-O	GLU409-N – THR406-O	**ARG410-N – THR407-O**	
THR407-OG1 – GLU545-OE2	GLU409-N – THR406-O	GLU409-N – ALA405-O	**ARG410-N – THR406-O**	**ARG410-NH1 – ASP432-OD1**	
GLU409-N – THR406-OG1	**ARG410-N – THR406**-O	ARG410-N – ALA406-O	**ARG410-N – ALA407-O**		
GLU409-N – THR406-O	**ARG410-N – THR407-O**	**ARG410-N – THR407-O**	**ARG410-NH1 – GLU545-OE1**		
ARG410-N – THR406-O	**ARG410-NH1 – GLU545-OE1**	ILE411-N – THR407-O	**ARG410-NH1 – GLU545-OE2**		
ARG410-N – THR407-O	**ARG410-NH1 – GLU545-OE2**	ILE411-N – LEU408-O	**ARG410-NH2 – GLU545-OE1**		
ARG410-NH2 – ALA405-O	ARG410-NH2 – ALA405-O		**ARG410-NH2 – GLU545-OE2**		
ILE411-N – THR407-O	**ARG410-NH2 – GLU545-OE1**		ILE411-N – LEU408-O		
ILE411-N – LEU408-O	**ARG410-NH2 – GLU545-OE2**				
	ILE411-N – LEU408-O				

Table S3: The average and the maximum number of hydrogen bonds over the entire simulations for each configuration calculated using VMD

State	Average number of bonds per frame	maximum number of bonds per frame
Light	45	60
Dark	40	57.5
tslight	45	65
tsdark	40	57.5
T406A light	40	57.5
T406A dark	40	57.5
T407A light	37.5	55
T407A dark	40	57.7
L408D light	37.5	55
L408D dark	37.5	55
R410P light	40	55
R410P dark	37.5	55

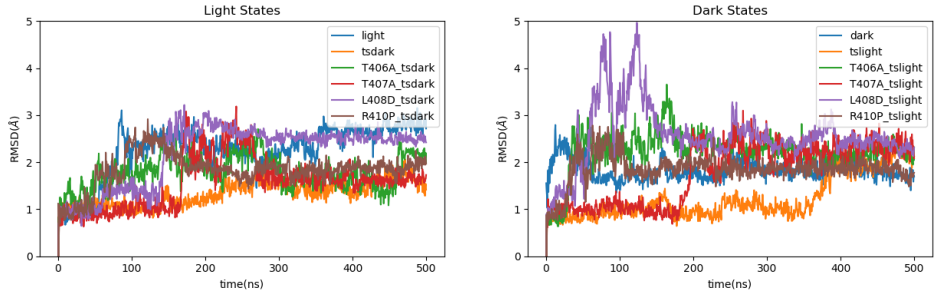

(a) **(b)**

Figure S1: RMSD of the trajectory for each configuration. a) RMSD for the wild type light state, transient dark states of both wild type and mutants; b) RMSD for the wild type dark state, transient light states of both wild type and mutants.

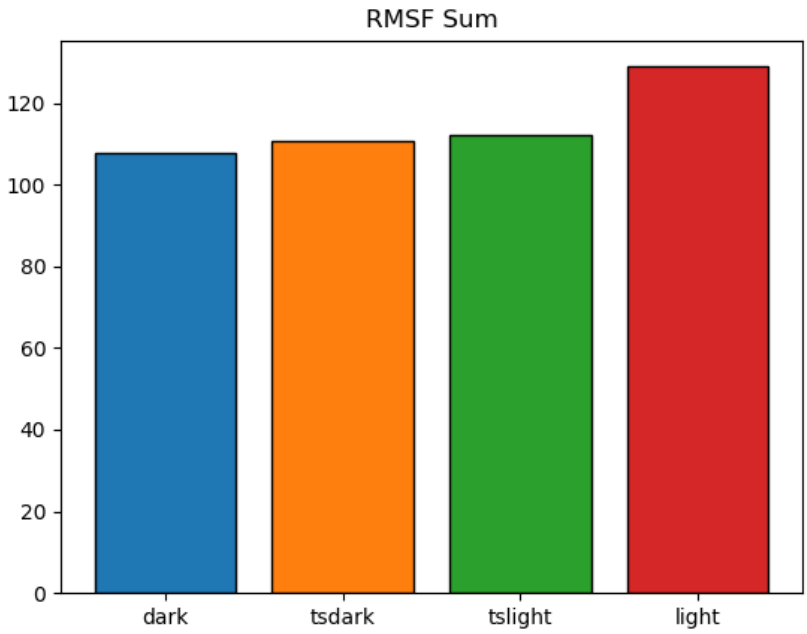

Figure S2: The sum of the RMSF values of the entire structure of *As*LOV2 for the wild type configurations.

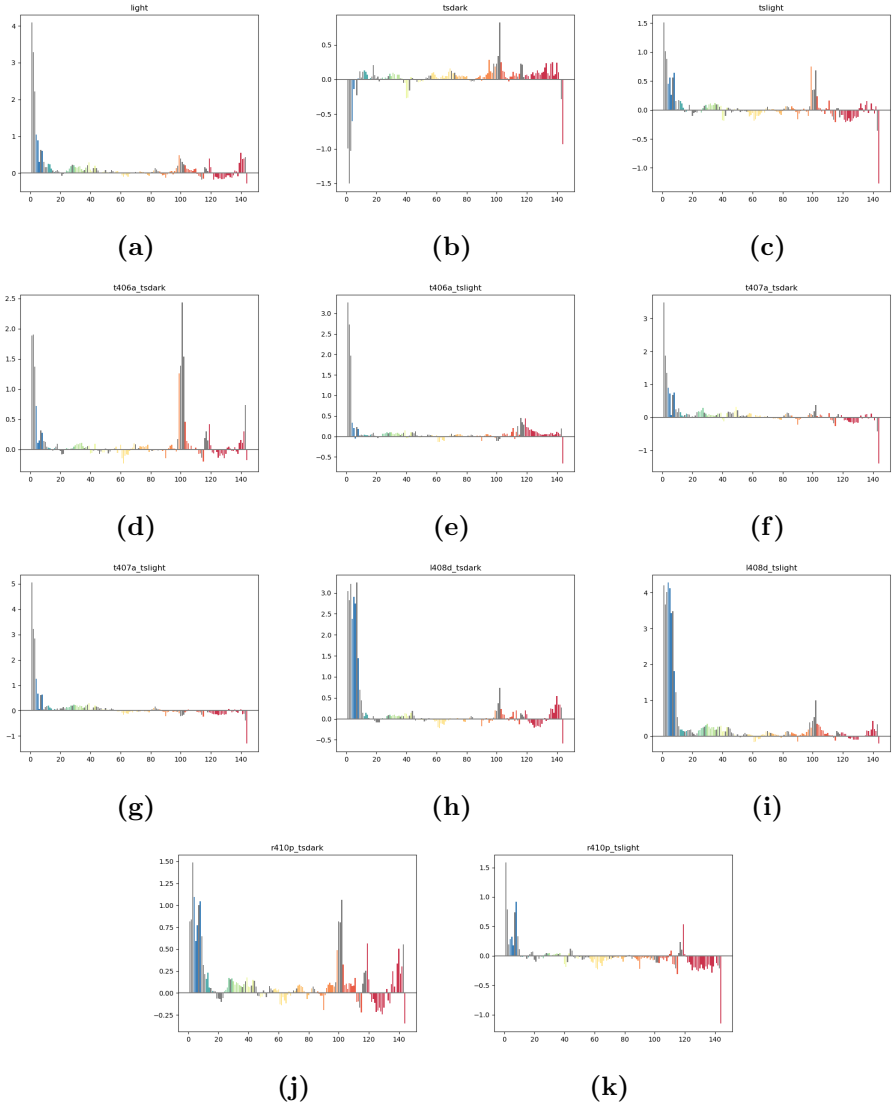

Figure S3: RMSF differences comparing to the wild type native dark state in wild type native light state, wild type and mutants transient states. For each configuration, the trajectory with the least deviation is plotted. a) Light state; b) Tsdark state; c) Tslight state; d) T406A tsdark state; e)T406A tslight; f) T407A tsdark; g) T407A tslight; h) L408D tsdark; i) L408D tslight; j) R410P tsdark; l) R410P tslight.

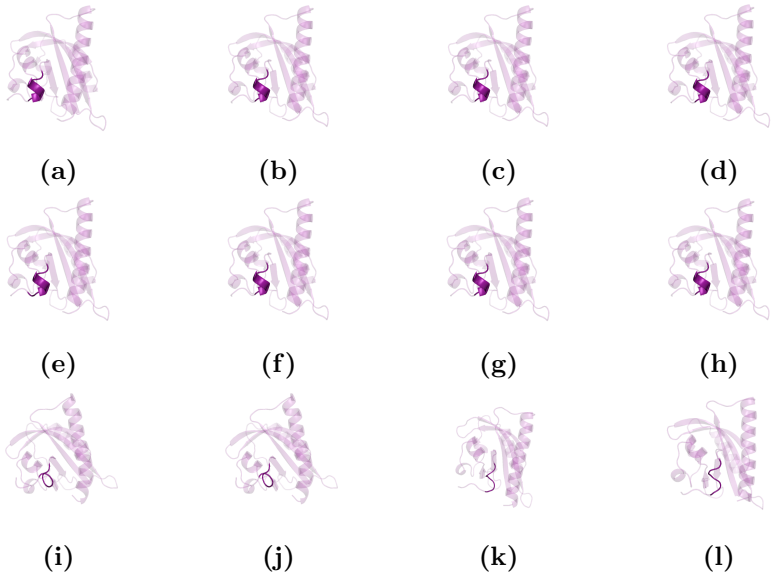

Figure S4: Helicity of the A'α helix shown in native, transient and mutant structures. The helical structure is maintained in all the states except for the states of the helicity-disrupting mutations (L408D and R410P). a) Light state; b) Dark state; c) Tslight state; d) Tsdark state; e)T406A tslight; f) T406A tsdark; g) T407A tslight; h) T407A tsdark; i) L408D tslight; j) L408D tsdark; k) R410P tslight; l) R410P tsdark.

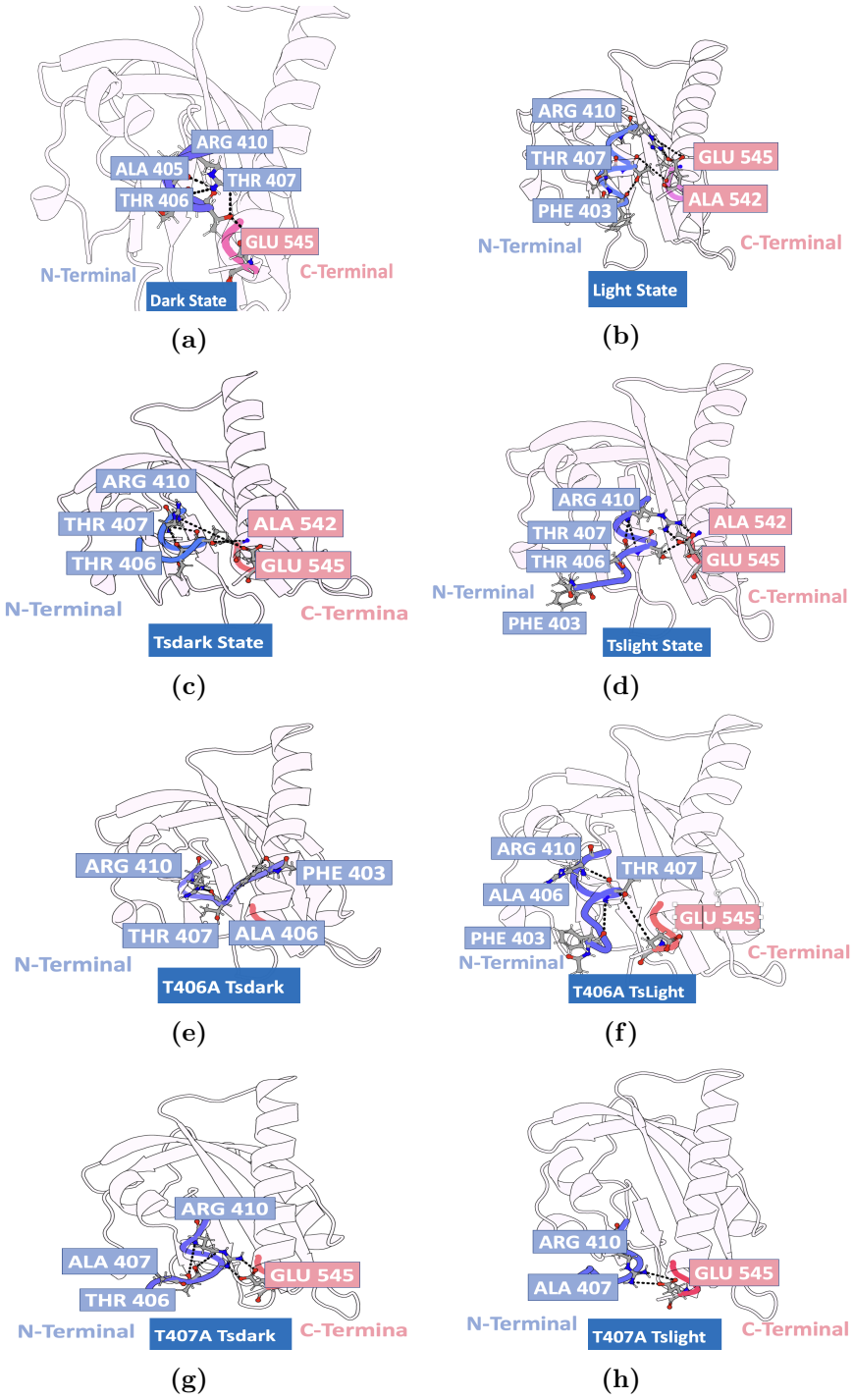

Figure S5: The hydrogen bonds formed with the A'α helix residues shown in native, transient and helicity enhancing mutants (T406A and T407A) structures. Phe403, Ala405, Thr406, Thr407, and Arg410 are the residues identified to contribute to the formation of the hydrogen bonds in most of the states. a) Dark state; b) Light state; c) Tsdark state; d) Tslight state; e)T406A tsdark; f) T406A tslight; g) T407A tsdark; h) T407A tslight.

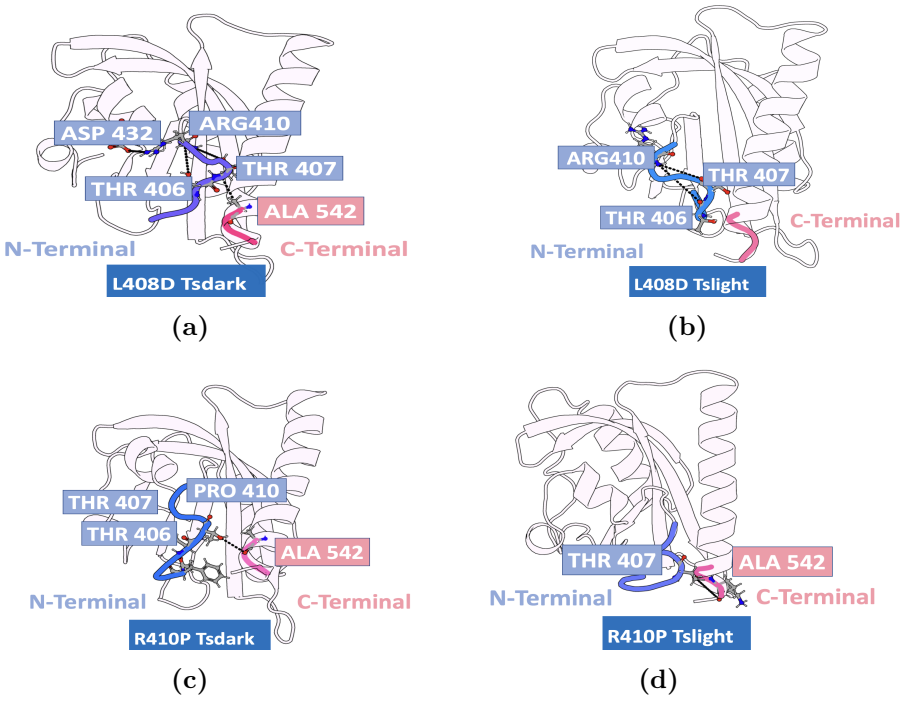

Figure S6: The hydrogen bonds formed with the A'α helix residues in helicity disrupting mutant structures (L408D and R410P). a) L408D tsdark; b) L408D tslight; c) R410P tsdark; d) R410P tslight.

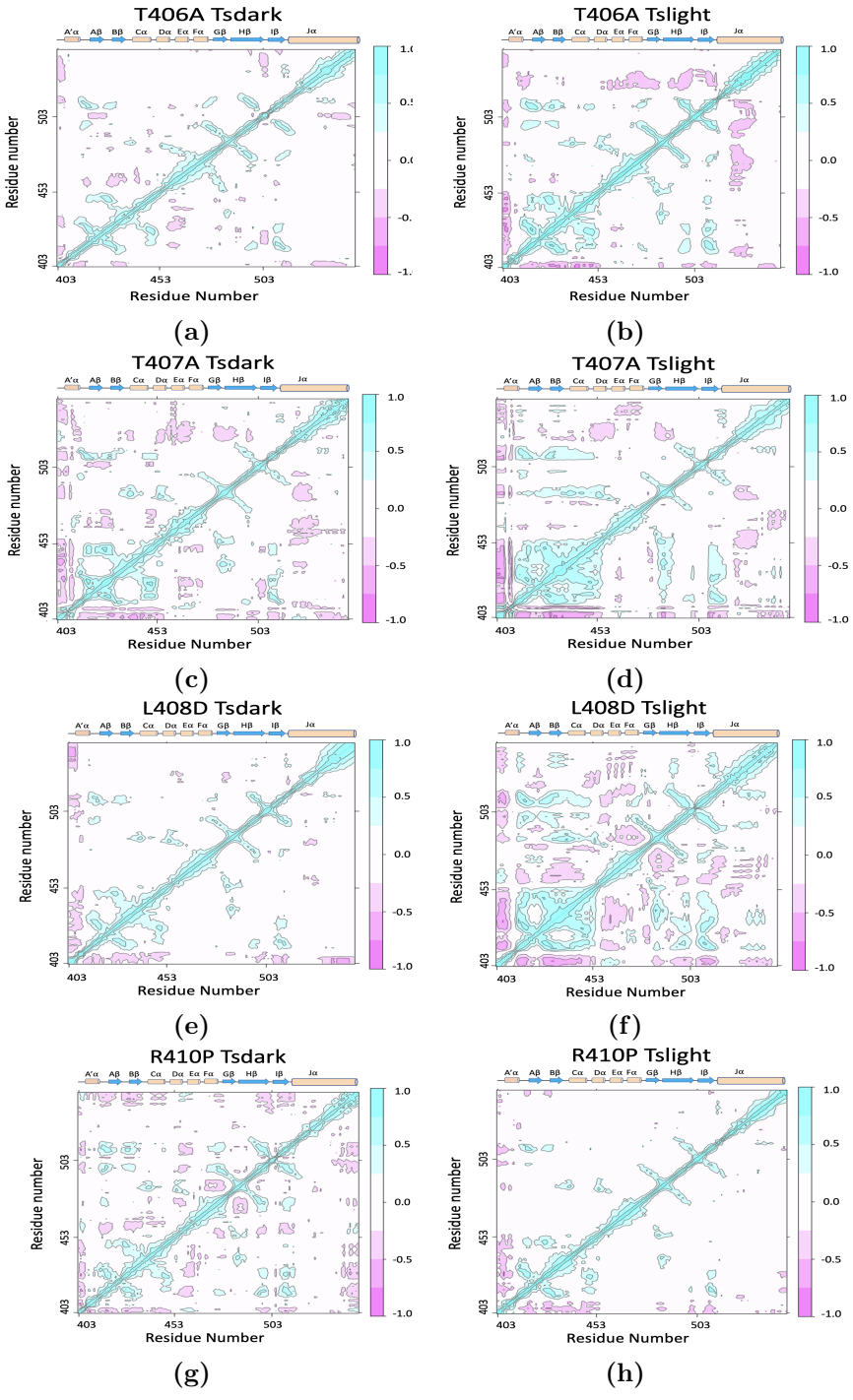

Figure S7: Cross-correlation among the residues of *As*LOV2 using Bio3D package [1] in the mutants. a)T406A tsdark state; b)T406A tslight; c) T407A tsdark; d) T407A tslight; e) L408D tsdark; f) L408D tslight; g) R410P tsdark; h) R410P tslight.

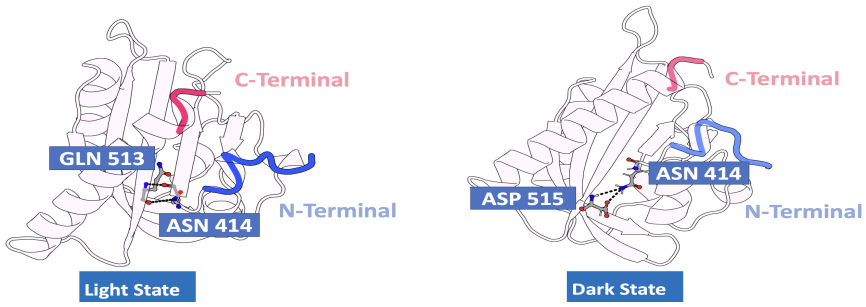

(a) **(b)**

Figure S8: The hydrogen bonds formed among Asn414, Gln513, and Asp515 in the wild type light and dark states. The transient hydrogen bond between Asn414 and Gln513 was attributed to the transfer of the allosteric signal from A'α helix to Jα helix upon photo activation of AsLOV2 [2]. a) Hydrogen bond formed between Asn414 and Gln513 in the light state configuration; b) Hydrogen bond formed between Asn414 and Asp515 in the dark state configuration.

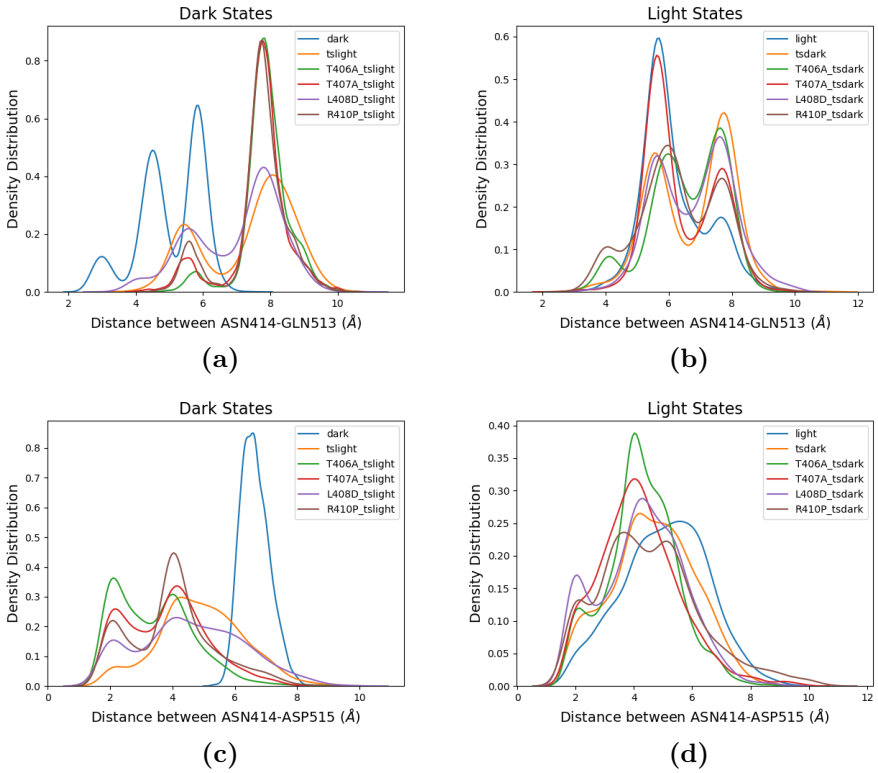

Figure S9: Distribution for distance between Asn414 (A'α helix) and Gln513 (Jα helix) and distance between Asn414 and Asp515 (Jα helix). a) Distance distribution between Asn414 and Gln513 in the configurations of the wild type dark state, and transient light states for wild type and four mutants; b) Distance distribution between Asn414 and Gln513 in the configurations of the wild type light state, and transient dark states for wild type and four mutants; c) Distance distribution between Asn414 and Asp515 in the configurations of the wild type dark state, and transient light states for wild type and four mutants; d) Distance distribution between Asn414 and Asp515 in the configurations of the wild type light state, and transient dark states for wild type and four mutants.

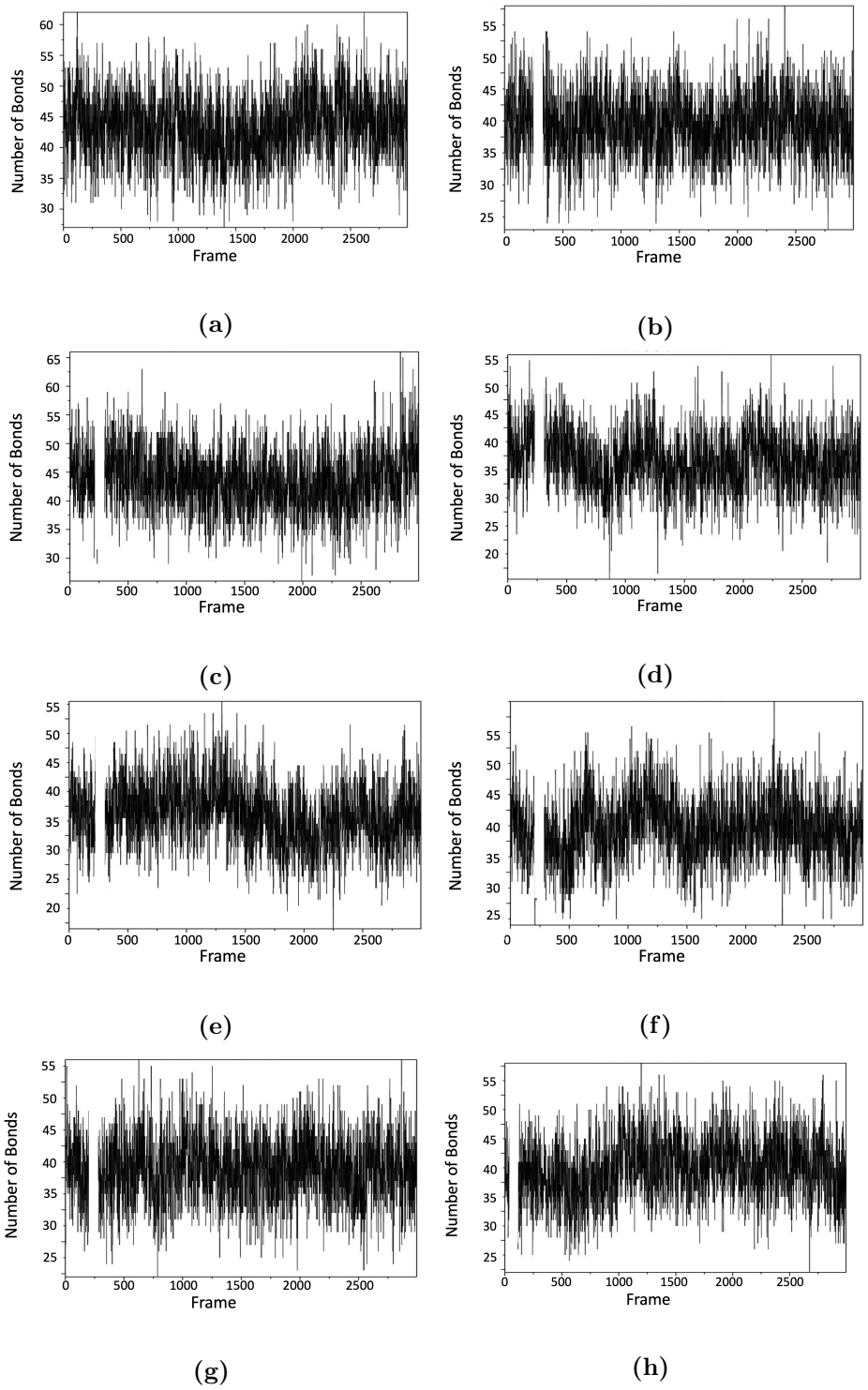

Figure S10: The number of hydrogen bonds for each simulation frame calculated using VMD. a) light; b) dark; c) tslight; d) tsdark; e) T406A tslight; f) T406A dark; g) T407A tslight; h) T407A tsdark.

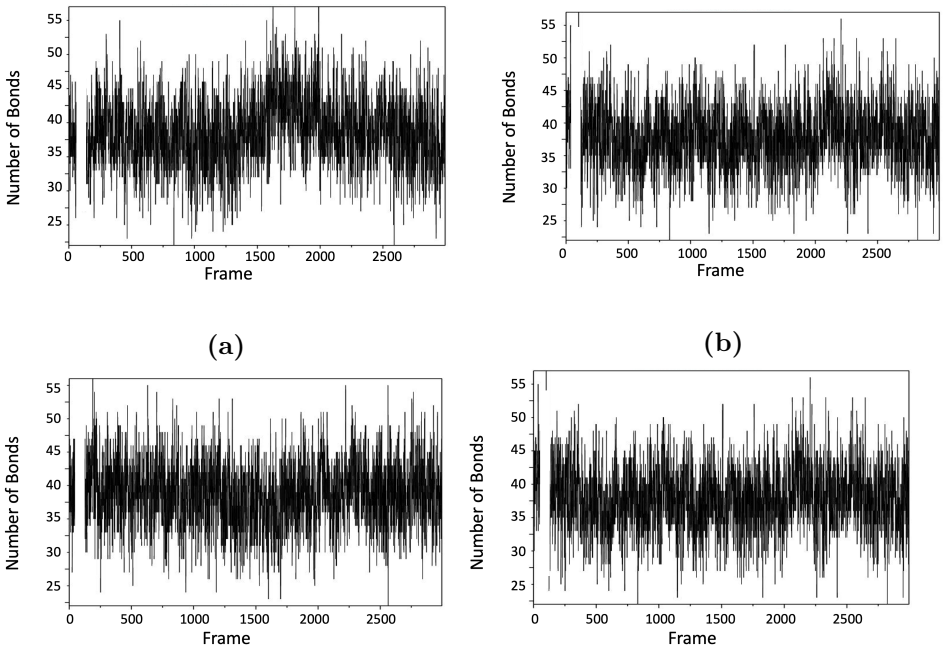

Figure S11: The number of hydrogen bonds for each simulation frame calculated using VMD. a)L408D tslight; b) L408D tsdark; c) R410P tslight; d) R410P tsdark.

References

[1] Barry J Grant, Lars Skjaerven, and Xin-Qiu Yao. The bio3d packages for structural bioinformatics. *Protein Science*, 30(1):20–30, 2021.

[2] James N Iuliano, Jinnette Tolentino Collado, Agnieszka A Gil, Pavithran T Ravindran, Andras Lukacs, SeungYoun Shin, Helena A Woroniecka, Katrin Adamczyk, James M Aramini, Uthama R Edupuganti, et al. Unraveling the mechanism of a lov domain optogenetic sensor: A glutamine lever induces unfolding of the jα helix. *ACS chemical biology*, 15(10):2752–2765, 2020.